Plasma Physics, Vol. 13, pp. 159 to 171. Pergamon Press 1971. Printed in Northern Ireland

DIFFUSION RESULTING FROM NONADIABATIC SCATTERING ON A HELICALLY PERTURBED FIELD IN A TORUS*

R. W. MOIR† and L. M. LIDSKY
Research Laboratory of Electronics and Department of Nuclear Engineering,
Massachusetts Institute of Technology, Cambridge, Mass. 02139, U.S.A.

(*Received* 6 *April* 1970)

Abstract—Resonant and nonresonant diffusion of electrons has been studied in a toroidal magnetic field with pulsed injection of electrons.

We have experimental evidence of the theoretical predictions of $B_\perp^{3/2}$ dependence of the diffusion coefficients in strong perturbation fields. We have observed the transition from $B_\perp^2$ to $B_\perp^{3/2}$ behavior for $B_\perp/B_0 < 1$ per cent where $B_\perp$ is the perturbing and B_0 the uniform magnetic field. Theoretical models based on unperturbed orbit calculations are shown to be invalid for surprisingly small values of $B_\perp/B_0$.

We have conducted measurements of nonresonant diffusion applicable to dissociation experiments in nonadiabatic traps. We find that the diffusion coefficient depends strongly on how nearly resonant the electron is with the perturbed field. For a 50 per cent change in effective perturbation frequency, the diffusion coefficient changes by a factor 1000.

Our results can be scaled to the problem of nonadiabatic trapping and dissociation of molecular ions. We infer the resulting nonresonant protons would have a lifetime against nonadiabatic scattering 10,000 times longer than the parent molecular ions.

1. INTRODUCTION

ONE way to trap an injected beam of charged particles in a static magnetic field is by nonadiabatic change of the magnetic moment, μ. In the case of a mirror trap one can achieve this by superimposing on the main field a spatially modulated field whose wavelength corresponds to the pitch length of an injected particle (SINEL'NIKOV *et al.*, 1960; WINGERSON, 1961). The behavior of these systems have been analyzed by (LAING, 1961; DREICER, 1962; WINGERSON, 1964; and ROBSON, 1965). The magnitude of this perturbation is typically a few percent of the main field. The particle will be acted upon by the field in a resonant manner and the magnetic moment may increase enough for the particle to be trapped on the first transit through the system. Since the particle was trapped by nonconservation of μ, it can also be lost by magnetic moment variations from one transit to the next, i.e. a random walk of the particle in μ-space. A good trapping perturbation is one that interacts strongly with particles injected through the loss cone and very weakly with trapped particles, which have undergone dissociation making them nonresonant.

Experiments have shown that the lifetime of the trapped particles in resonant traps is typically of the order 10–50 transits through the perturbed field (DREICER *et al.*, 1962; ROBSON *et al.*, 1967). A somewhat different type of nonadiabatic trap succeeded in achieving 450 transits (HUBERT, 1967). This lifetime is too short to allow accumulation of interesting densities for plasma studies. However if there is a strong break-up mechanism one can trap molecular ions which are resonant and produce, by dissociation, nonresonant ions. If the life time of the nonresonant ions is long enough, interesting densities of hot plasma can be produced.

* This work was supported by the U.S. Atomic Energy Commission under Contract No. AT(30-1)-3980.

† Present address: Lawrence Radiation Laboratory, University of California, Livermore, Calif. 94551, U.S.A.

We first address ourselves to the verification of theoretical models for predicting the lifetime of both resonant and nonresonant particles in order to predict the behavior of molecular ion and atomic ions in a nonadiabatic trap.

Theory of nonadiabatic scattering

The theory of nonadiabatic scattering is based on the random walk problem. Figure 1 shows the system to be analyzed and Fig. 2 the coordinate system definitions.

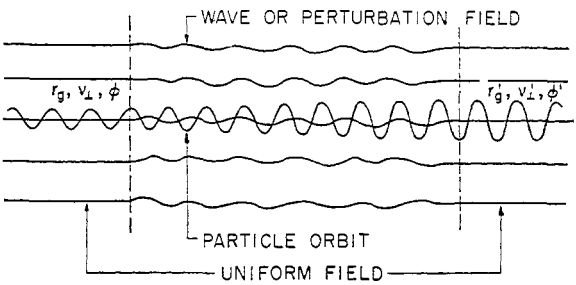

FIG. 1.—Schema of system to be analyzed. The perturbation region is limited in spatial extent. The particles enter from the left. Configuration space diffusion is not considered.

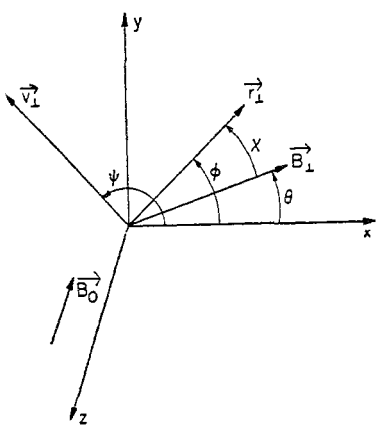

FIG. 2.—Coordinate system. The z coordinate axis is antiparallel to the unperturbed magnetic field.

The particle of speed V_0 is specified by r_g, the guiding center position; $V_\perp$ the velocity transverse to B; and ψ, the phase angle in velocity space. The particles enter the perturbation from the left and leave to the right. The field is assumed to have no X or Y dependence, thus configuration space diffusion is independent of velocity space diffusion. We will treat V space diffusion only because it is the dominant loss mechanism for the systems under discussion. On each pass through the perturbed field the perpendicular velocity changes by $\Delta V_\perp = V_\perp - V_{\perp 0}$. This step in velocity space is determined by the parameters at the entrance of the perturbed region, i.e. by $V_{\perp 0}$ and ϕ_0, where ϕ is the angular position (phase). After the particle leaves the perturbation region, it undergoes many cyclotron gyrations either in orbiting a toroidal field or in reflection from a field gradient before re-entrance to the perturbation. Two particles with the same value of ϕ but slightly different values of $V_\perp$ will thus become phase mixed. The phase randomization is essentially complete in

laboratory systems and the probability of possessing any particular phase at the entrance is given by $P(\phi) = (2\pi)^{-1}$.

If the velocity space steps are small enough the Fokker–Planck equation describes the evolution of a distribution of particles with distribution function $f(v_\perp, v_\parallel, \phi, t)$;

$$\frac{\partial f}{\partial t} = -\frac{\partial}{\partial V_\perp}\left\langle \frac{\Delta V_\perp}{\tau} \right\rangle f + \frac{1}{2}\frac{\partial^2}{\partial V_\perp{}^2}\left\langle \frac{(\Delta V_\perp)^2}{\tau} \right\rangle f \tag{1}$$

where $\Delta v_\perp$ and $(\Delta v_\perp)^2$ refer to changes in $v_\perp$ in a single encounter with the perturbation and τ is the mean time between such encounters. We have neglected terms of order $(\Delta v_\perp{}^3/\tau)$ in equation (1) and defined

$$(\Delta V_\perp)^n = \left[\int_0^\tau \frac{\mathrm{d}v_t}{\mathrm{d}t}\,\mathrm{d}t\right]^n \tag{2}$$

and the averaging operator by

$$\langle(\ \ )\rangle \equiv \frac{1}{2\pi}\int_0^{2\pi} (\ \ )\,\mathrm{d}\phi_0. \tag{3}$$

In equation (2), we calculate the step in $v_\perp$ for a particular value of initial phase, ϕ_0; the problem at this point is single valued and deterministic. In equation (3), we invoke phase randomization. One can show that when

$$\left\langle \frac{\Delta V_\perp}{\tau} \right\rangle = \frac{\partial}{\partial V_\perp}\left\langle \frac{(\Delta v_\perp)^2}{2\tau} \right\rangle \tag{4}$$

equation (1) reduces to a simple diffusion equation

$$\frac{\partial f}{\partial t} = \frac{\partial}{\partial v_\perp}\left\langle \frac{(\Delta v_\perp)^2}{\tau} \right\rangle \frac{\partial}{\partial V_\perp} f. \tag{5}$$

It has been shown (DUNNETT, 1968, 1966) that when the velocity steps are large the diffusion equation approach can be used and when the steps are small, nonrandom behavior (invariants of the motion) may inhibit diffusion, thus our nonresonant diffusion estimates may be too big.

The problem here is the calculation of the various coefficients $(\Delta v_\perp)^n$ to determine the magnitude of the scattering and whether or not the scattering may be described by a diffusion equation. It will turn out that a more complicated formulation of the equation describing the evolution of the distribution function must be invoked for resonant interactions.

In the coordinate system of Fig. 2, the equation of motion for a single particle is

$$\frac{\mathrm{d}V_z}{\mathrm{d}t} = -\frac{e}{m} V_\theta B_\perp \cos\chi + \frac{e}{m} V_r B_\theta \cos\chi. \tag{6}$$

When $B_\perp$ is of order B_θ and V_r is small compared to V_θ, as is generally the case for weak perturbations, the second term in equation (6) may be neglected, and $v_\perp \simeq v_\theta$. The necessary condition is

$$\frac{P}{r_\perp}\frac{B_\perp}{B_0} M \ll 1$$

where P is the field pitch, $r_\perp$ the larmor radius and M the number of field periods for which the particle is near resonance. In this approximation, equation (6) reduces to

$$\frac{dv_\perp}{dz} = \frac{e}{m} B_\perp \cos\chi \tag{7}$$

where χ is the angle between the local direction of the perturbation field and the particle coordinate vector. The spatial gradient of χ is simply the difference between the particle and field spatial rotation rates;

$$\frac{d\chi}{dz} = \frac{\omega_0}{v_z} - \frac{2\pi}{P}. \tag{8}$$

When the rates of rotation of field and particle are nearly equal, i.e. when $d\chi/dz \approx 0$, the particle is *resonant* with the field. The resonance is the spatial analogue of the more common time domain cyclotron resonance. The increased complexity occurs because the change in orbit with interaction leads to nonlinearities not present in spatially uniform cases. The expression for the coefficients of equation (2) now reduces to

$$(\Delta v_\perp)^n = \left[\int_0^L \frac{e}{m} B_\perp(z) \cos\chi(z)\, dz\right]^n \tag{9}$$

where L is the length of the perturbed region.

Equation (9) is troublesome because χ depends on $\Delta v_\perp$ through the variation of v_z. We choose to solve equation (9) for $\Delta v_\perp$ by iteration. On the first iteration we assume $v_z = \text{const} = v_{z0}$ and solve for $\chi(z)$ and then obtain $\Delta v_\perp$ from equation (9). This initial iteration uses unperturbed orbits and is generally known as first order perturbation theory. Quasilinear theory also uses unperturbed orbits and is equivalent to our first iteration of the equations for $\Delta v_\perp$.

Define $\Delta v_{\perp 0}$ to be the result of integrating equation (9) along the unperturbed orbit $v_{\perp 0}$. We expand

$$\Delta V_\perp = \Delta V_\perp|_0 + \frac{1}{2}\frac{\partial}{\partial V_{\perp 0}} (\Delta V_\perp|_0)^2 + \ldots. \tag{10}$$

Phase averaging equation (10) then gives

$$\langle \Delta V_\perp \rangle = \frac{1}{2}\frac{\partial}{\partial v_{\perp 0}} \langle \Delta V_\perp|_0^2 \rangle \tag{10a}$$

(the first term vanishes because of the symmetry properties of the unperturbed orbit).

The second iteration is performed by allowing v_z to vary according to equation (8).

$$\frac{\omega_0}{v_z} = \frac{\omega_0}{v_{z0}(1 + \Delta v_z/v_{z0})} \simeq \frac{\omega_0}{v_{z0}}\left(1 + \frac{v_\perp}{{v_{z0}}^2}\Delta v_\perp\right). \tag{11}$$

One then calculates a new value of χ

$$\chi_1 = \chi_0 + \int_0^z \left\{\frac{\omega_0}{v_{z0}} - \frac{2\pi}{P} + \frac{\omega_0 v_\perp}{{v_{z0}}^3}\Delta v_\perp\right\} dz'. \tag{12}$$

The change in χ from the first iteration to the second is a measure of how closely the

unperturbed orbit approximates the true orbit

$$\Delta\chi(z) = \frac{\omega_0 v_\perp}{V_{z0}^3}\int_0^z \Delta v_\perp(z')\,dz' . \tag{13}$$

When $\langle(\Delta\chi/2\pi)^2\rangle$ is small the first iteration is valid and when it is of order unity the second iteration is required (CLARKE, 1966). With the new value of $\Delta\chi$ one can calculate the second iterative $\Delta v_\perp$:

$$\Delta v_\perp = \int_0^L \frac{eB_{\perp(z)}}{m}\cos\left[\chi_1(z)\right]dz . \tag{14}$$

Equation (9) has been evaluated in this approximation for two cases of interest: the 'corkscrew' and a constant pitch helical perturbation.

Case 1: *varying pitch helical field, 'corkscrew'*

The perturbation field is a varying pitch helical field 'corkscrew' specified by its pitch p and field strength $B_\perp$ (WINGERSON, 1964).

$$B_\perp = B_{\perp 0}\sin(\pi z/L) \tag{15a}$$

$$p(z) = p_0\left[1 - \alpha^2\cos^4\left(\frac{\pi z}{2L}\right)\right]^{1/2} . \tag{15b}$$

The parameter α^2 is the 'windup ratio' and is numerically equal to the normalized magnetic moment at the perturbation exit for a resonant particle (Wingerson presents a complete discussion of the corkscrew trap and a rigorous derivation of first order theory for very weak perturbations). For given values of ω_0 and $v_\perp$, resonance will occur at a position z_0 where

$$p(z_0) = 2\pi v_z(z_0)/\omega_0. \tag{16}$$

The particle sees a force which oscillates rapidly except near z_0, the resonance point. At the resonance point, χ is stationary and a saddle point integration of equation (9) can be performed. The result of this first order (unperturbed orbit) calculation is (WINGERSON, 1964)

$$\langle(\Delta v_\perp)^2\rangle = \frac{1}{2\pi}\int_0^{2\pi}\left\{Re\int_0^L \frac{e}{m}B_\perp(z)\,e^{i\chi(z)}\,dz\right\}^2 d\chi_0 \tag{17a}$$

$$= Av_0^2F(z_0)\left(\frac{B_\perp}{B_0}\right)^2 \tag{17b}$$

where v_0 is the particle speed and the dependence on the field strength has been emphasized. A and F are constants determined by the geometry of the field. The number of transits of the perturbation required for velocity space diffusive escape through the loss cone defined by θ_l is

$$N = \theta_l^2/\langle(\Delta v_\perp/v_0)^2\rangle \tag{18}$$

which implies that when $B_\perp/B_0$ is small enough for equation (17) to be valid, then the number of transits is proportional to $(B_\perp/B_0)^{-2}$.

When $B_\perp/B_0$ is large enough, the iterative solution must be used. Clarke (CLARKE,

op. cit.) has calculated the iteration (equation (13)) for the field of equations (15) and finds $N \propto B_{\perp}^{-3/2}$.

The effect of the field on the particle is to 'push' a particle out of resonant field regions giving a longer lifetime than predicted on the basis of unperturbed orbit calculations. Dupree (Dupree, 1966) has found the same behavior for electrostatic waves, that is $\langle(\Delta v_{\perp})^2/\tau\rangle \propto E^{3/2}$ where E is the electric field of the wave.

Case 2: *constant pitch helical field*

The field is specified by

$$B_{\perp} = B_{\perp 0} \sin(\pi z/L) \tag{19}$$

$$p(z) = p_0 = \text{constant}. \tag{20}$$

For this case the integral of equation (9) can be performed and the average taken. The diffusion coefficient for weak perturbations then becomes

$$\left\langle \frac{(\Delta v_{\perp})^2}{v_0^2} \right\rangle = AF(\gamma_0) \left(\frac{B_{\perp}}{B_0}\right)^2 \tag{21}$$

and the number of transits required for escape is

$$N = \theta_i^2/AF(\gamma_0) \left(\frac{B_{\perp}}{B_0}\right)^2 \tag{22}$$

where

$$A = \left(\frac{\pi L}{\gamma_0}\right)^2$$

$$\gamma_0 = \frac{\omega_0}{v_{z0}} - \frac{2\pi}{p_0}$$

and

$$F(\gamma) = \frac{1 + \cos(\gamma L)}{[\pi^2 - (\gamma L)^2]^2}.$$

2. EXPERIMENTAL ARRANGEMENT AND RESULTS

In order to determine the diffusion coefficients experimentally, a device was built which satisfied the assumptions required by the theory described above. A toroidal field was used to allow unidirectional passage through the perturbation and to provide a long path length for phase randomization between successive transits. A related experiment was performed using a toroidal nonadiabatic trap by (Slabospitskii, 1965).

A schematic of the torus and injection system is shown in Fig. 3 and a photograph of the device in Fig. 4. The electron gun supplies 50 μamp d.c. at 1500 V. When the inflector voltage is off, the electron beam simply follows the field lines into a suitably placed anode. To inject an electron bunch into the system, the inflector plates are turned on rapidly (800 V with 20 nsec rise time). The beam then moves with essentially the $(\mathbf{E} \times \mathbf{B})/B^2$ velocity towards the magnetic axis. The potential is adjusted so that when the particle has reached the end of the inflector plates it is on the magnetic axis. The inflector pulse is switched off before the leading edge of the bunch has gone all the way around the torus. The transit time at 1500 eV is 325 nsec for the

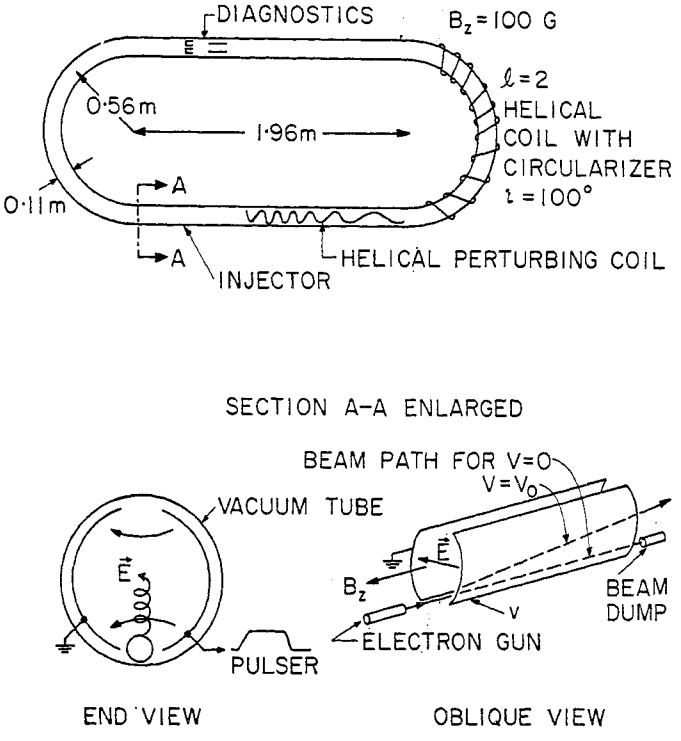

FIG. 3.—Toroidal scattering apparatus. The coils used to produce a small vertical field in the U-bends are not shown. The enlarged view shows the inflector used to inject the pulsed beam into the system. The injector pulse voltage was chosen so that the beam was on the magnetic axis exiting the plates.

7·45 m circumference torus. A 280 nsec injection time was usually employed which resulted in the injection of an electron bunch of 6·4 m length. The resulting 1 m gap fills as the electrons circulate because of dispersion in their axial velocity.

The principal diagnostics were the charge collector and cylindrical capacitive pickup probes shown in Fig. 5. The charge collector plate was held sufficiently positive to retain secondary electrons and was enclosed in a grounded cage.

In Fig. 6 we show probe results which indicate the kind of measurements possible in this device. When the leading and trailing edges of the injected electron bunch pass through the detector a voltage is induced on the probe on each transit around the torus. This is a measure of the axial velocity. The oscillations damp out as the gap between the leading and trailing edges of the beam close. This is a sensitive measure of the axial velocity spread. In addition to the rapid oscillation one notes a lower frequency oscillation which is produced by the beam being slightly off axis and precessing azimuthally due to the rotational transform which was measured to be 50°.

When the beam is injected off axis the charge collector signal is also modulated due to the rotational transform carrying the beam towards the detector then away from it. Figure 6(c) shows this modulation effect where the time between peaks is T_{transit} (360°/transform angle). This is another method of measuring rotational transform as well as particle lifetime.

The circulating electrons diffuse in velocity and configuration space as a result of the combined action of many perturbations including, for example, noncancelled

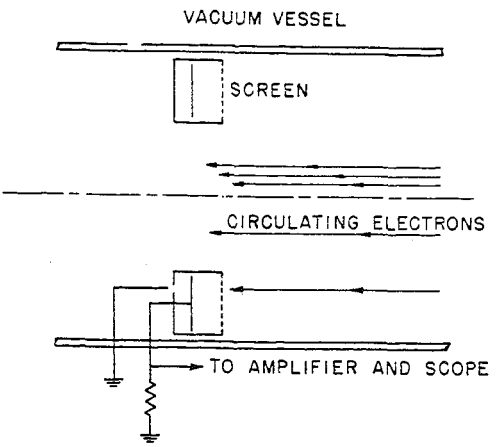

(a) CHARGE COLLECTOR

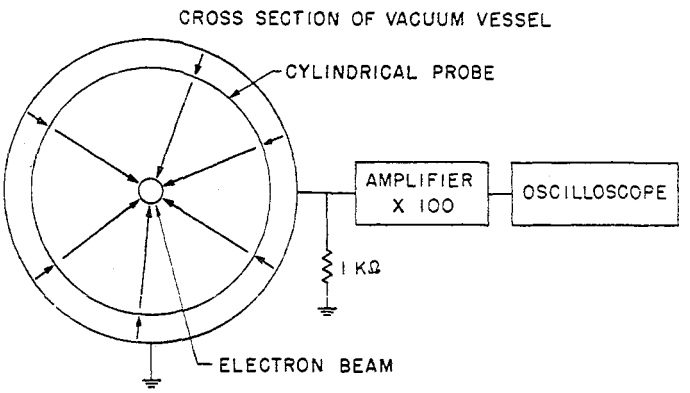

(b) ELECTROSTATIC PROBE

FIG. 5.—Charge collector and capacitive probe. The charge collector measures particle loss directly whereas the cylindrical probe is sensitive to time and space variations of the circulating charge.

toroidal drifts, gas scattering, and nonadiabatic interactions with the magnetic field. The drifts are cancelled by an $l = 2$ helical coil with 100° rotational transform on one U-bend and a vertical field on the other. The resulting drift cancellation is very velocity dependent and the major losses are attributable to the velocity space loss cone—when $(v_\perp/v_0)^2 \approx 0{\cdot}7$, the particles intercept the charge collector. The effective loss cone edge $v_{\perp l}$ is at much smaller values of $v_\perp/v_0$ because of the rapid increase in U-bend drifts with $v_\perp$. We estimate $(v_{\perp l}/v_0)^2 \simeq 0{\cdot}1$. The measured diffusion coefficient is thus averaged over the region $0 \leqslant v_\perp/v_0 \leqslant 0{\cdot}3$. From the theory of random walks, the number of transits of the torus performed by a circulating electron is given by $N = v_{\perp l}^2/\langle(\Delta v_\perp)^2\rangle$. We determine the number of transits by measuring the current collected in the annular charge collector as a function of elapsed time after injection.

The electrons are injected with $v_\perp = 0$. This distribution rapidly evolves into a velocity space 'normal mode' which exhibits a single exponential time constant for diffusion into the loss cone. The time constant $N(B_\perp)$ is observed for a given perturbation field, $B_\perp$, and, with otherwise identical conditions, for $B_\perp = 0$. For random

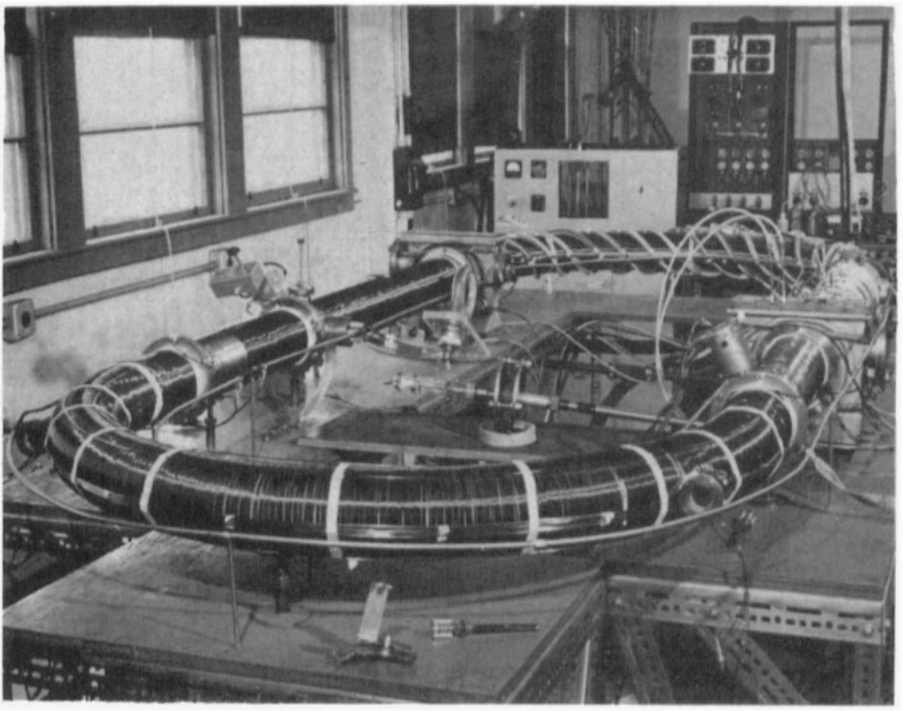

FIG. 4.—Photograph of the toroidal scattering experiment. The 'l-windings' are on the further U-bend. The drift correcting windings are on the torus itself. The conductors running parallel to the minor axis on the inside and outside of the torus were used to cancel the vertical component of the geomagnetic field.

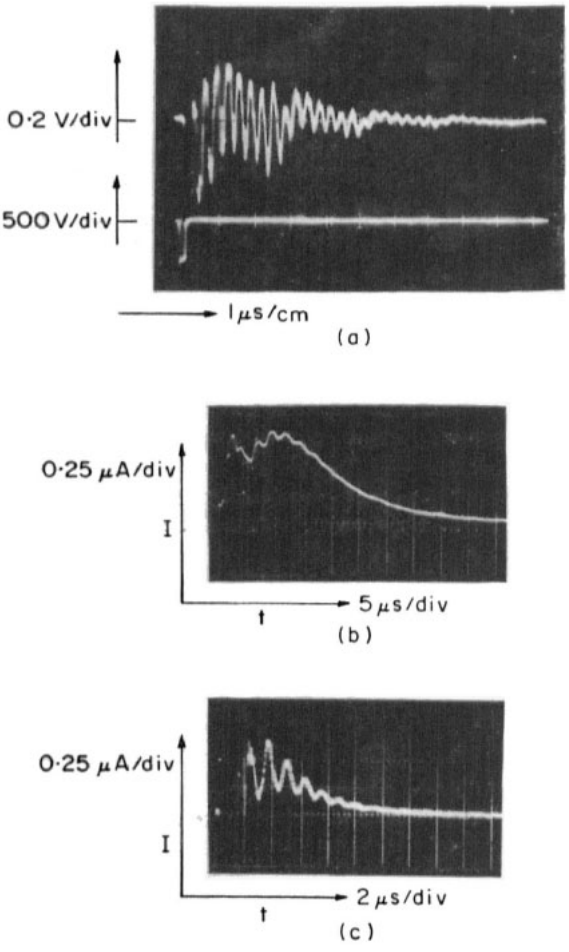

FIG. 6.—(a) Capacitive probe signal. The lower trace shows the injection pulse and the upper trace the probe response to the circulation beam. The ~1 m gap in the circulating beam is seen to close in ~25 transits of the system (e.g. the velocity spread is less than 4–5 per cent). (b) Charge collector signal. This shows the typical exponential decay of the loss rate after an initial rapid change which the higher order terms in the density distribution decay away. (c) Charge collector signal for off-axis injection. The frequency of the large oscillations compared to the transit frequency is a measure of the rotational transform.

scattering, the effective lifetime against loss caused solely by the perturbation field, N is just

$$N^{-1} = N(B_\perp)^{-1} - N(0)^{-1} \tag{23}$$

Equation (23) assumes that the effects of the variable field, $B_\perp$, and those of all the other perturbations are statistically independent. This assumption is easily justified for small values of $B_\perp$ and is unimportant for large values when $N(B_\perp)^{-1}$ is the dominant term. The symbol 'N' is used for the time constant as a reminder that the number of transits of the torus, and hence the number of interactions with the variable nonadiabatic field is proportional to the residence time only when $(v_{\perp i}/v_0)^2 \ll 1$.

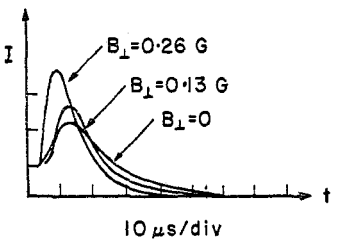

FIG. 7.—Electron loss current vs. time. The figure is an overlay of oscilloscope traces for three different values of perturbation field.

Figure 7 shows the charge collector current as a function of time for different perturbation fields. The positive sloped portion of the curves occurs during the initial period before the distribution attains the normal mode. The curve following the peak is very accurately defined by a simple exponential time constants; viz. i.e. $I = I_0 \exp(-t/\tau)$. The area under the curve is proportional to the total injected current and was monitored throughout the experiment to verify that no electrons were being lost in unobserved regions of the apparatus. In the figure, the decay time observed for $B_\perp = 0$ corresponds to an exponential loss constant of 14·5 μsec or $\approx$45 transits. This number took on values in the range $40 \leqslant N(0) \leqslant 220$ transits during the course of the experiments depending on such things as the vacuum system base pressure or accuracy of adjustment of the vertical correction coils. This value was also monitored frequently during the course of the experiment.

The figure also demonstrates convincingly that relatively small perturbing fields can have quite noticeable and easily measurable effects. Curves of this type were the raw data for the experiments summarized below.

The first perturbation structure investigated was the corkscrew field of equations (15a) and (15b) with starting pitch of 13·4 cm, total length of 100 cm, and windup ratio, α^2, equal to 0·80. The toroidal field was held constant and $B_\perp$ was varied. Figure 8 shows the experimental data. The resonance scattering obviously varies more slowly with perturbation amplitude than the square law prediction of first order perturbation theory. Within experimental error, the diffusion coefficient varies with the 3/2 power of perturbation strength predicted by Clarke and by Dupree. This figure is the first experimental verification of this behavior.

In Fig. 9 we show data for $B_\perp$ constant and B_z varied to change the resonant point. The solid line shows the theoretical prediction (equation (18)). Electrons with $v_\perp = 0$ resonate at $z_0 = 0$ for 61·2 G. The resonance point shifts toward shorter pitch length

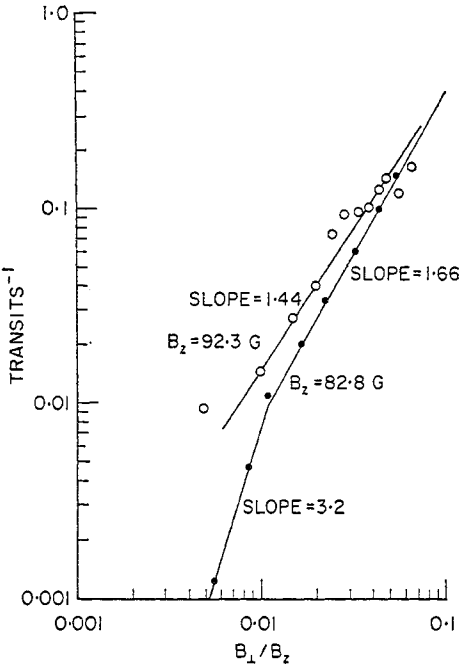

FIG. 8.—Inverse transits vs. perturbation field amplitude. The slope of the line is a direct measure of the power law dependence of the 'diffusion coefficient'.

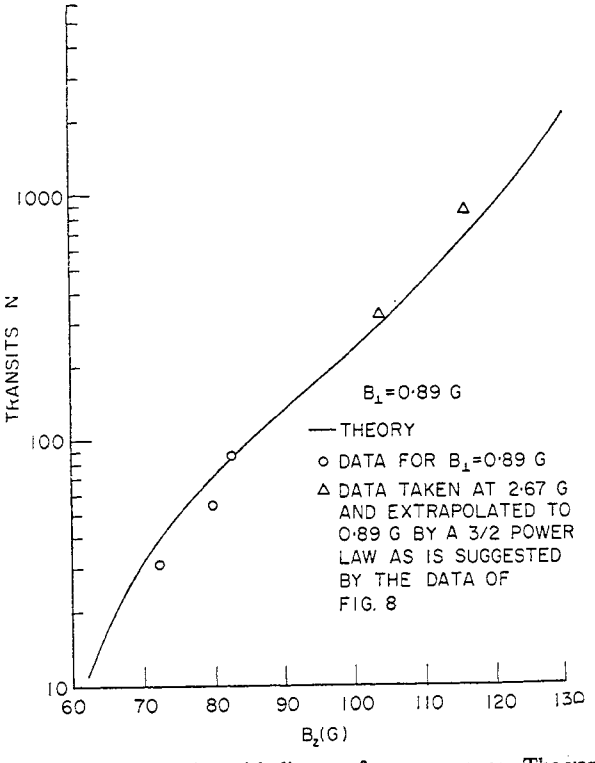

FIG. 9.—Variation of scattering with distance from resonance. The variation of B shifts the resonant point along the corkscrew axis.

as B_z increases and attains $z_0 = L$ at 133 G. At higher fields, the electrons are never resonant. The figure shows that the nonlinear theory must be used even for weak scattering—the life-time is equivalent to 2000 transits for $(B_\perp/B_0) = 7 \times 10^{-3}$ but the variation of $\langle(\Delta v_\perp)^2\rangle$ still follows a 3/2 power low variation.

There are two effects of importance in the study of near-resonant scattering. One is the role of perturbation field strength in introducing important nonlinear effects into the actual orbit and the other is the order of agreement between the cyclotron frequency and the doppler shifted field perturbation. Figure 10 shows the results of an experiment designed to measure the 'resonance width'. The perturbation field used was that described by equations (19) and (20) with $P_0 = 11{\cdot}7$ cm and peak field of 2·62 G. We point out that the resonance of this eight-turn helix is surprisingly sharp

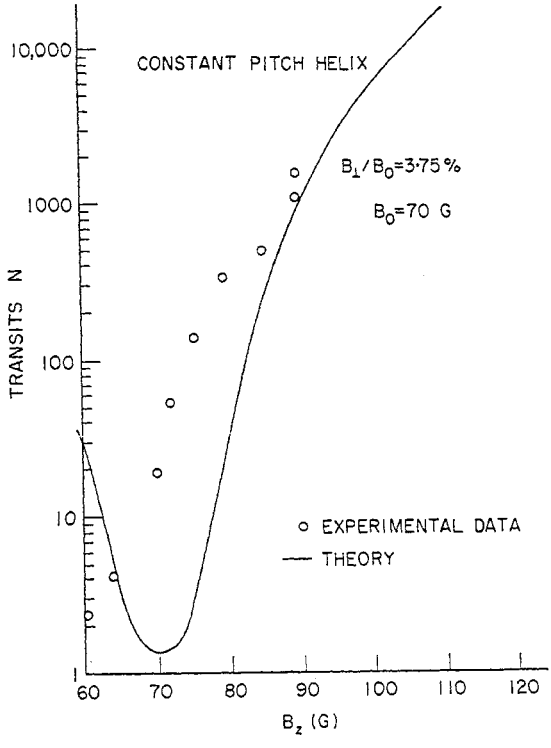

FIG. 10.—Number of transits as a function of field strength for a constant pitch helix. The resonant point is at 70 G. The experimental data lies above the theoretical curve for all B above 70 G. The large deviation near exact resonance indicates that second order nonlinear effects become very important when spatial variations do not limit the resonant length.

and that the lifetime against scattering varies by a factor of nearly 10^3 for a 50 per cent change in the resonance parameter. The scattering near resonance varied as $B_\perp$, approximately as $B_\perp^{3/2}$ for intermediate fields, and as $B_\perp^2$ for axial fields in excess of 75 G. The measured lifetime was always greater than that predicted by linear theory which justifies our use of linear theory in the next section as a conservative estimate of particle lifetime against scattering. This increased lifetime in the nonlinear regime was predicted by Clarke and by Dupree. It follows from the simple fact that the particle will tend to spend less time in regions were the zero-order interaction is

strong because it is in precisely those regions where its orbit is being most rapidly modified.

3. APPLICATION OF RESULTS TO NONADIABATIC MOLECULAR ION TRAPPING

The diffusion coefficients were measured in a torus. However they are characteristic of the perturbed field, and not of the toroidal geometry. Therefore we can apply our results to the behavior of particles in a nonadiabatic magnetic mirror trap.

We consider the problem of trapping a molecular ion beam in a magnetic mirror device. We assume a perturbed field designed to increase the magnetic moment sufficiently on the first pass to trap the injected particles. As the molecular ions move back and forth through the perturbation from one mirror to the other they diffuse in velocity space and are lost within a few tens of transits. A large fraction of the molecular ions will break up into atomic ions before the molecular ions are lost by nonadiabatic scattering if there is a strong break-up mechanism. One such mechanism is dissociation for example on a 10^{12}/cc cold plasma produced by electron cyclotron heating (LAZAR *et al.*, 1967).

For illustration we pick a system for which the experimental measurements are directly applicable. As long as all dimensions are scaled linearly and the B field is scaled to give the same orbit sizes then our results from the experiment using electrons will be directly applicable to predictions of ion behavior. We consider a perturbation of the form of equations (19) and (20); $B_\perp = 375$ G, $B_z = 10$ kG, $P_0 = 35$ cm, $R = 5$ = mirror ratio, 3 m long.

Experiments have shown that the normalized magnetic moment after a single traversal of the perturbation is equal to 0·23. The injected particles are thus trapped in a system with the assumed mirror ratio. In this case, the molecular ion lifetime before scattering into the loss cone, N, will be equivalent to at least 10 transits (DREICER, *op. cit.*; ROBSON, *op. cit.*).

The fraction of the input current I, that will be dissociated within the trap of length l by collisions with cross-section σ on the cold plasma of density n_0 is just $[1 - \exp(-Nl\sigma n_0)]$. From Fig. 11, we see that the residence time of the dissociated particles will be greater than 10^5 transits. For reasonable values of the parameters ($l = 100$ m, $n_0 = 10^{12}$/cm^3, $\sigma_0 = 10^{-16}$ cm^2) the fractional breakup is of order unity and so the line density in the input beam is multiplied by a factor of 10^5. For an input beam of 1 amp of 200 keV H_2^+, this yields a trapped proton line density of $1{\cdot}4 \times 10^{15}$/cm. Clearly, the limiting density will be set by charge transfer scattering on the cold plasma background. In effect, we are claiming that a resonant perturbation used in conjunction with a moderately strong plasma trapping medium can result in essentially complete trapping of the input beam and further that the presence of the resonant perturbation will have negligible effect on the no longer resonant dissociated particles.

The very long lifetime of the dissociated particles is attributable to the fact that the magnetic moment is well conserved for off-resonance particles. This would not be true if the magnetic field of the perturbation had sharp gradients because then other nonadiabaticities would be introduced for all particles in the system. This was the reason for the much shorter lifetime measured for nonresonant particles by DREICER *et al.*

4. CONCLUSIONS

We have shown that the theoretical model based on unperturbed orbits is valid for calculating the diffusion coefficient when the lifetimes are long, and 'conservative' when the lifetime is short. The lifetimes are long for nonresonant diffusion and for very weak resonant fields, in which cases the diffusion coefficient is proportional to $B_\perp{}^2$. As the perturbation field strength is increased the orbit begins to deviate from the unperturbed orbit. For strong fields the equations must be iterated a second time in order to more closely approximate the exact particle orbit. For strong fields we have experimentally verified for the first time that the diffusion coefficient is proportional to $B_\perp^{3/2}$.

One of our results leads to a re-examination of the possibilities of molecular ion trapping and subsequent dissociation into energetic ions. For a particular system analyzed we predict essentially complete trapping of a beam injected into a cold background plasma.

REFERENCES

CLARKE J. F. and LIDSKY L. M. (1970) *Physics Fluids*, **13**, 1580.

DREICER H., KARR H. J., KNAPP E. A., PHILLIPS J. A., STOVALL, E. J. JR. and TUCK J. L. (1962) *Nucl. Fusion Suppl.* **1**, 299.

DUNNETT D. A., LAING E. W. and TAYLOR J. B. (1968) *J. math. Phys.* **9**, 1819.

DUNNETT D. A. and LAING E. W. (1966) *Plasma Phys. (J. nucl. Energy*, Part C) **8**, 399.

DUPREE T. H. (1966) *Physics Fluids* **9**, 1773.

HUBERT P. and TOUCHE J. (1967) *Physics Fluid* **10**, 1676.

LAING E. W. and ROBSON A. E. (1961) *Plasma Phys. (J. nucl. Energy*, Part C) **3**, 146.

LAZAR N., GUEST G. and DANDLE W. (1967) *Oak Ridge, Tennessee Rep. No.* ORNL-4080.

ROBSON A. E. and TAYLOR J. B. (1965) *Physics Fluids* **11**, 2026.

ROBSON A. E., AITKEN K. L., ALDCROFT D. A., LLOYD O. and MORTON A. H. (1967) *Plasma Phys. (J. nucl. Energy*, Part C) **9**, 121.

SINEL'NIKOV K. D., RUTKEVICK B. N. and FEDORCHENKO V. D. (1960) *Soviet Phys. Tech. Phys. 5*, 229.

SLABOSPITSKII A. P. and FEDORCHENKO V. D. (1965) *Inter Atomic Conf. Plasma Phys. and Controlled Nucl. Fusion Res. Culham U.K.*, 6–10 Sept (1965), Paper CTO/105.

WINGERSON R. C. (1961) *Phys. Rev. Lett.* **6**, 446.

WINGERSON R. C., DUPREE T. H. and ROSE D. J. (1964) *Physics Fluids* **7**, 1475.